

A Direct Top-Quark Width Measurement from Lepton + Jets Events at CDF II

T. Aaltonen,²² B. Álvarez González^{v,10} S. Amerio,⁴² D. Amidei,³³ A. Anastassov,³⁷ A. Annovi,¹⁸ J. Antos,¹³ G. Apollinari,¹⁶ J.A. Appel,¹⁶ A. Apresyan,⁴⁷ T. Arisawa,⁵⁶ A. Artikov,¹⁴ J. Asaadi,⁵² W. Ashmanskas,¹⁶ B. Auerbach,⁵⁹ A. Aurisano,⁵² F. Azfar,⁴¹ W. Badgett,¹⁶ A. Barbaro-Galtieri,²⁷ V.E. Barnes,⁴⁷ B.A. Barnett,²⁴ P. Barria^{ee,45} P. Bartos,¹³ M. Bauce^{cc,42} G. Bauer,³¹ F. Bedeschi,⁴⁵ D. Beecher,²⁹ S. Behari,²⁴ G. Bellettini^{dd,45} J. Bellinger,⁵⁸ D. Benjamin,¹⁵ A. Beretvas,¹⁶ A. Bhatti,⁴⁹ M. Binkley^{*,16} D. Bisello^{cc,42} I. Bizjak^{ii,29} K.R. Bland,⁵ C. Blocker,⁷ B. Blumenfeld,²⁴ A. Bocci,¹⁵ A. Bodek,⁴⁸ D. Bortoletto,⁴⁷ J. Boudreau,⁴⁶ A. Boveia,¹² B. Brau^{a,16} L. Brigliadori^{bb,6} A. Brisuda,¹³ C. Bromberg,³⁴ E. Brucken,²² M. Bucciantonio^{dd,45} J. Budagov,¹⁴ H.S. Budd,⁴⁸ S. Budd,²³ K. Burkett,¹⁶ G. Busetto^{cc,42} P. Bussey,²⁰ A. Buzatu,³² S. Cabrera^{x,15} C. Calancha,³⁰ S. Camarda,⁴ M. Campanelli,³⁴ M. Campbell,³³ F. Canelli^{12,16} A. Canepa,⁴⁴ B. Carls,²³ D. Carlsmith,⁵⁸ R. Carosi,⁴⁵ S. Carrillo^{k,17} S. Carron,¹⁶ B. Casal,¹⁰ M. Casarsa,¹⁶ A. Castro^{bb,6} P. Catastini,¹⁶ D. Cauz,⁵³ V. Cavaliere^{ee,45} M. Cavalli-Sforza,⁴ A. Cerri^{f,27} L. Cerrito^{q,29} Y.C. Chen,¹ M. Chertok,⁸ G. Chiarelli,⁴⁵ G. Chlachidze,¹⁶ F. Chlebana,¹⁶ K. Cho,²⁶ D. Chokheli,¹⁴ J.P. Chou,²¹ W.H. Chung,⁵⁸ Y.S. Chung,⁴⁸ C.I. Ciobanu,⁴³ M.A. Ciocci^{ee,45} A. Clark,¹⁹ D. Clark,⁷ G. Compostella^{cc,42} M.E. Convery,¹⁶ J. Conway,⁸ M. Corbo,⁴³ M. Cordelli,¹⁸ C.A. Cox,⁸ D.J. Cox,⁸ F. Crescioli^{dd,45} C. Cuenca Almenar,⁵⁹ J. Cuevas^{v,10} R. Culbertson,¹⁶ D. Dagenhart,¹⁶ N. d'Ascenzo^{t,43} M. Datta,¹⁶ P. de Barbaro,⁴⁸ S. De Cecco,⁵⁰ G. De Lorenzo,⁴ M. Dell'Orso^{dd,45} C. Deluca,⁴ L. Demortier,⁴⁹ J. Deng^{c,15} M. Deninno,⁶ F. Devoto,²² M. d'Errico^{cc,42} A. Di Canto^{dd,45} B. Di Ruzza,⁴⁵ J.R. Dittmann,⁵ M. D'Onofrio,²⁸ S. Donati^{dd,45} P. Dong,¹⁶ T. Dorigo,⁴² K. Ebina,⁵⁶ A. Elagin,⁵² A. Eppig,³³ R. Erbacher,⁸ D. Errede,²³ S. Errede,²³ N. Ershaidat^{aa,43} R. Eusebi,⁵² H.C. Fang,²⁷ S. Farrington,⁴¹ M. Feindt,²⁵ J.P. Fernandez,³⁰ C. Ferrazza^{ff,45} R. Field,¹⁷ G. Flanagan^{r,47} R. Forrest,⁸ M.J. Frank,⁵ M. Franklin,²¹ J.C. Freeman,¹⁶ I. Furic,¹⁷ M. Gallinaro,⁴⁹ J. Galyardt,¹¹ J.E. Garcia,¹⁹ A.F. Garfinkel,⁴⁷ P. Garosi^{ee,45} H. Gerberich,²³ E. Gerchtein,¹⁶ S. Giagu^{gg,50} V. Giakoumopoulou,³ P. Giannetti,⁴⁵ K. Gibson,⁴⁶ C.M. Ginsburg,¹⁶ N. Giokaris,³ P. Giomini,¹⁸ M. Giunta,⁴⁵ G. Giurgiu,²⁴ V. Glagolev,¹⁴ D. Glenzinski,¹⁶ M. Gold,³⁶ D. Goldin,⁵² N. Goldschmidt,¹⁷ A. Golossanov,¹⁶ G. Gomez,¹⁰ G. Gomez-Ceballos,³¹ M. Goncharov,³¹ O. González,³⁰ I. Gorelov,³⁶ A.T. Goshaw,¹⁵ K. Goulianos,⁴⁹ A. Gresele,⁴² S. Grinstein,⁴ C. Grosso-Pilcher,¹² R.C. Group,¹⁶ J. Guimaraes da Costa,²¹ Z. Gunay-Unalan,³⁴ C. Haber,²⁷ S.R. Hahn,¹⁶ E. Halkiadakis,⁵¹ A. Hamaguchi,⁴⁰ J.Y. Han,⁴⁸ F. Happacher,¹⁸ K. Hara,⁵⁴ D. Hare,⁵¹ M. Hare,⁵⁵ R.F. Harr,⁵⁷ K. Hatakeyama,⁵ C. Hays,⁴¹ M. Heck,²⁵ J. Heinrich,⁴⁴ M. Herndon,⁵⁸ S. Hewamanage,⁵ D. Hidas,⁵¹ A. Hocker,¹⁶ W. Hopkins^{9,16} D. Horn,²⁵ S. Hou,¹ R.E. Hughes,³⁸ M. Hurwitz,¹² U. Husemann,⁵⁹ N. Hussain,³² M. Hussein,³⁴ J. Huston,³⁴ G. Introzzi,⁴⁵ M. Iori^{gg,50} A. Ivanov^{o,8} E. James,¹⁶ D. Jang,¹¹ B. Jayatilaka,¹⁵ E.J. Jeon,²⁶ M.K. Jha,⁶ S. Jindariani,¹⁶ W. Johnson,⁸ M. Jones,⁴⁷ K.K. Joo,²⁶ S.Y. Jun,¹¹ T.R. Junk,¹⁶ T. Kamon,⁵² P.E. Karchin,⁵⁷ Y. Kato^{n,40} W. Ketchum,¹² J. Keung,⁴⁴ V. Khotilovich,⁵² B. Kilminster,¹⁶ D.H. Kim,²⁶ H.S. Kim,²⁶ H.W. Kim,²⁶ J.E. Kim,²⁶ M.J. Kim,¹⁸ S.B. Kim,²⁶ S.H. Kim,⁵⁴ Y.K. Kim,¹² N. Kimura,⁵⁶ S. Klimenko,¹⁷ K. Kondo,⁵⁶ D.J. Kong,²⁶ J. Konigsberg,¹⁷ A. Korytov,¹⁷ A.V. Kotwal,¹⁵ M. Kreps,²⁵ J. Kroll,⁴⁴ D. Krop,¹² N. Krumnack^{l,5} M. Kruse,¹⁵ V. Krutelyov^{d,52} T. Kuhr,²⁵ M. Kurata,⁵⁴ S. Kwang,¹² A.T. Laasanen,⁴⁷ S. Lami,⁴⁵ S. Lammel,¹⁶ M. Lancaster,²⁹ R.L. Lander,⁸ K. Lannon^{u,38} A. Lath,⁵¹ G. Latino^{ee,45} I. Lazzizzera,⁴² T. LeCompte,² E. Lee,⁵² H.S. Lee,¹² J.S. Lee,²⁶ S.W. Lee^{w,52} S. Leo^{dd,45} S. Leone,⁴⁵ J.D. Lewis,¹⁶ C.-J. Lin,²⁷ J. Linacre,⁴¹ M. Lindgren,¹⁶ E. Lipeles,⁴⁴ A. Lister,¹⁹ D.O. Litvintsev,¹⁶ C. Liu,⁴⁶ Q. Liu,⁴⁷ T. Liu,¹⁶ S. Lockwitz,⁵⁹ N.S. Lockyer,⁴⁴ A. Loginov,⁵⁹ D. Lucchesi^{cc,42} J. Lueck,²⁵ P. Lujan,²⁷ P. Lukens,¹⁶ G. Lungu,⁴⁹ J. Lys,²⁷ R. Lysak,¹³ R. Madrak,¹⁶ K. Maeshima,¹⁶ K. Makhoul,³¹ P. Maksimovic,²⁴ S. Malik,⁴⁹ G. Manca^{b,28} A. Manousakis-Katsikakis,³ F. Margaroli,⁴⁷ C. Marino,²⁵ M. Martínez,⁴ R. Martínez-Ballarín,³⁰ P. Mastrandrea,⁵⁰ M. Mathis,²⁴ M.E. Mattson,⁵⁷ P. Mazzanti,⁶ K.S. McFarland,⁴⁸ P. McIntyre,⁵² R. McNulty^{i,28} A. Mehta,²⁸ P. Mehtala,²² A. Menzione,⁴⁵ C. Mesropian,⁴⁹ T. Miao,¹⁶ D. Mietlicki,³³ A. Mitra,¹ H. Miyake,⁵⁴ S. Moed,²¹ N. Moggi,⁶ M.N. Mondragon^{k,16} C.S. Moon,²⁶ R. Moore,¹⁶ M.J. Morello,¹⁶ J. Morlock,²⁵ P. Movilla Fernandez,¹⁶ A. Mukherjee,¹⁶ Th. Muller,²⁵ P. Murat,¹⁶ M. Mussini^{bb,6} J. Nachtman^{m,16} Y. Nagai,⁵⁴ J. Naganoma,⁵⁶ I. Nakano,³⁹ A. Napier,⁵⁵ J. Nett,⁵⁸ C. Neu^{z,44} M.S. Neubauer,²³ J. Nielsen^{e,27} L. Nodulman,² O. Norniella,²³ E. Nurse,²⁹ L. Oakes,⁴¹ S.H. Oh,¹⁵ Y.D. Oh,²⁶ I. Oksuzian,¹⁷ T. Okusawa,⁴⁰ R. Orava,²² L. Ortolan,⁴ S. Pagan Griso^{cc,42} C. Pagliarone,⁵³ E. Palencia^{f,10} V. Papadimitriou,¹⁶ A.A. Paramonov,² J. Patrick,¹⁶ G. Pauletta^{hh,53} M. Paulini,¹¹ C. Paus,³¹ D.E. Pellett,⁸ A. Penzo,⁵³ T.J. Phillips,¹⁵ G. Piacentino,⁴⁵ E. Pianori,⁴⁴ J. Pilot,³⁸ K. Pitts,²³ C. Plager,⁹ L. Pondrom,⁵⁸ K. Potamianos,⁴⁷ O. Poukhov^{*,14} F. Prokoshin^{y,14} A. Pronko,¹⁶ F. Ptohos^{h,18} E. Pueschel,¹¹ G. Punzi^{dd,45} J. Pursley,⁵⁸ A. Rahaman,⁴⁶ V. Ramakrishnan,⁵⁸ N. Ranjan,⁴⁷ I. Redondo,³⁰ P. Renton,⁴¹ M. Rescigno,⁵⁰ F. Rimondi^{bb,6} L. Ristori^{45,16} A. Robson,²⁰ T. Rodrigo,¹⁰ T. Rodriguez,⁴⁴ E. Rogers,²³ S. Rolli,⁵⁵ R. Roser,¹⁶ M. Rossi,⁵³ F. Ruffini^{ee,45} A. Ruiz,¹⁰ J. Russ,¹¹ V. Rusu,¹⁶ A. Safonov,⁵² W.K. Sakumoto,⁴⁸ L. Santi^{hh,53}

L. Sartori,⁴⁵ K. Sato,⁵⁴ V. Saveliev^{t,43} A. Savoy-Navarro,⁴³ P. Schlabach,¹⁶ A. Schmidt,²⁵ E.E. Schmidt,¹⁶ M.P. Schmidt*,⁵⁹ M. Schmitt,³⁷ T. Schwarz,⁸ L. Scodellaro,¹⁰ A. Scribano^{ee,45} F. Scuri,⁴⁵ A. Sedov,⁴⁷ S. Seidel,³⁶ Y. Seiya,⁴⁰ A. Semenov,¹⁴ F. Sforza^{dd,45} A. Sfyrla,²³ S.Z. Shalhout,⁸ T. Shears,²⁸ P.F. Shepard,⁴⁶ M. Shimojima^{s,54} S. Shiraishi,¹² M. Shochet,¹² I. Shreyber,³⁵ A. Simonenko,¹⁴ P. Sinervo,³² A. Sissakian*,¹⁴ K. Sliwa,⁵⁵ J.R. Smith,⁸ F.D. Snider,¹⁶ A. Soha,¹⁶ S. Somalwar,⁵¹ V. Sorin,⁴ P. Squillacioti,¹⁶ M. Stanitzki,⁵⁹ R. St. Denis,²⁰ B. Stelzer,³² O. Stelzer-Chilton,³² D. Stentz,³⁷ J. Strologas,³⁶ G.L. Strycker,³³ Y. Sudo,⁵⁴ A. Sukhanov,¹⁷ I. Suslov,¹⁴ K. Takemasa,⁵⁴ Y. Takeuchi,⁵⁴ J. Tang,¹² M. Tecchio,³³ P.K. Teng,¹ J. Thom^{g,16} J. Thome,¹¹ G.A. Thompson,²³ E. Thomson,⁴⁴ P. Ttito-Guzmán,³⁰ S. Tkaczyk,¹⁶ D. Toback,⁵² S. Tokar,¹³ K. Tollefson,³⁴ T. Tomura,⁵⁴ D. Tonelli,¹⁶ S. Torre,¹⁸ D. Torretta,¹⁶ P. Totaro^{hh,53} M. Trovato^{ff,45} Y. Tu,⁴⁴ N. Turini^{ee,45} F. Ukegawa,⁵⁴ S. Uozumi,²⁶ A. Varganov,³³ E. Vataga^{ff,45} F. Vázquez^{k,17} G. Velev,¹⁶ C. Vellidis,³ M. Vidal,³⁰ I. Vila,¹⁰ R. Vilar,¹⁰ M. Vogel,³⁶ G. Volpi^{dd,45} P. Wagner,⁴⁴ R.L. Wagner,¹⁶ T. Wakisaka,⁴⁰ R. Wallny,⁹ S.M. Wang,¹ A. Warburton,³² D. Waters,²⁹ M. Weinberger,⁵² W.C. Wester III,¹⁶ B. Whitehouse,⁵⁵ D. Whiteson^{c,44} A.B. Wicklund,² E. Wicklund,¹⁶ S. Wilbur,¹² F. Wick,²⁵ H.H. Williams,⁴⁴ J.S. Wilson,³⁸ P. Wilson,¹⁶ B.L. Winer,³⁸ P. Wittich^{g,16} S. Wolbers,¹⁶ H. Wolfe,³⁸ T. Wright,³³ X. Wu,¹⁹ Z. Wu,⁵ K. Yamamoto,⁴⁰ J. Yamaoka,¹⁵ T. Yang,¹⁶ U.K. Yang^{p,12} Y.C. Yang,²⁶ W.-M. Yao,²⁷ G.P. Yeh,¹⁶ K. Yi^{m,16} J. Yoh,¹⁶ K. Yorita,⁵⁶ T. Yoshida^{j,40} G.B. Yu,¹⁵ I. Yu,²⁶ S.S. Yu,¹⁶ J.C. Yun,¹⁶ A. Zanetti,⁵³ Y. Zeng,¹⁵ and S. Zucchelli^{bb6}
(CDF Collaboration[†])

The CDF Collaboration

¹*Institute of Physics, Academia Sinica, Taipei, Taiwan 11529, Republic of China*

²*Argonne National Laboratory, Argonne, Illinois 60439, USA*

³*University of Athens, 157 71 Athens, Greece*

⁴*Institut de Fisica d'Altes Energies, Universitat Autònoma de Barcelona, E-08193, Bellaterra (Barcelona), Spain*

⁵*Baylor University, Waco, Texas 76798, USA*

⁶*Istituto Nazionale di Fisica Nucleare Bologna, ^{bb}University of Bologna, I-40127 Bologna, Italy*

⁷*Brandeis University, Waltham, Massachusetts 02254, USA*

⁸*University of California, Davis, Davis, California 95616, USA*

⁹*University of California, Los Angeles, Los Angeles, California 90024, USA*

¹⁰*Instituto de Fisica de Cantabria, CSIC-University of Cantabria, 39005 Santander, Spain*

¹¹*Carnegie Mellon University, Pittsburgh, Pennsylvania 15213, USA*

¹²*Enrico Fermi Institute, University of Chicago, Chicago, Illinois 60637, USA*

¹³*Comenius University, 842 48 Bratislava, Slovakia; Institute of Experimental Physics, 040 01 Kosice, Slovakia*

¹⁴*Joint Institute for Nuclear Research, RU-141980 Dubna, Russia*

¹⁵*Duke University, Durham, North Carolina 27708, USA*

¹⁶*Fermi National Accelerator Laboratory, Batavia, Illinois 60510, USA*

¹⁷*University of Florida, Gainesville, Florida 32611, USA*

¹⁸*Laboratori Nazionali di Frascati, Istituto Nazionale di Fisica Nucleare, I-00044 Frascati, Italy*

¹⁹*University of Geneva, CH-1211 Geneva 4, Switzerland*

²⁰*Glasgow University, Glasgow G12 8QQ, United Kingdom*

²¹*Harvard University, Cambridge, Massachusetts 02138, USA*

²²*Division of High Energy Physics, Department of Physics,*

University of Helsinki and Helsinki Institute of Physics, FIN-00014, Helsinki, Finland

²³*University of Illinois, Urbana, Illinois 61801, USA*

²⁴*The Johns Hopkins University, Baltimore, Maryland 21218, USA*

²⁵*Institut für Experimentelle Kernphysik, Karlsruhe Institute of Technology, D-76131 Karlsruhe, Germany*

²⁶*Center for High Energy Physics: Kyungpook National University,*

Daegu 702-701, Korea; Seoul National University, Seoul 151-742,

Korea; Sungkyunkwan University, Suwon 440-746,

Korea; Korea Institute of Science and Technology Information,

Daejeon 305-806, Korea; Chonnam National University, Gwangju 500-757,

Korea; Chonbuk National University, Jeonju 561-756, Korea

²⁷*Ernest Orlando Lawrence Berkeley National Laboratory, Berkeley, California 94720, USA*

²⁸*University of Liverpool, Liverpool L69 7ZE, United Kingdom*

²⁹*University College London, London WC1E 6BT, United Kingdom*

³⁰*Centro de Investigaciones Energeticas Medioambientales y Tecnológicas, E-28040 Madrid, Spain*

³¹*Massachusetts Institute of Technology, Cambridge, Massachusetts 02139, USA*

³²*Institute of Particle Physics: McGill University, Montréal, Québec,*
Canada H3A 2T8; Simon Fraser University, Burnaby, British Columbia,

Canada V5A 1S6; University of Toronto, Toronto, Ontario,

Canada M5S 1A7; and TRIUMF, Vancouver, British Columbia, Canada V6T 2A3

- ³³University of Michigan, Ann Arbor, Michigan 48109, USA
³⁴Michigan State University, East Lansing, Michigan 48824, USA
³⁵Institution for Theoretical and Experimental Physics, ITEP, Moscow 117259, Russia
³⁶University of New Mexico, Albuquerque, New Mexico 87131, USA
³⁷Northwestern University, Evanston, Illinois 60208, USA
³⁸The Ohio State University, Columbus, Ohio 43210, USA
³⁹Okayama University, Okayama 700-8530, Japan
⁴⁰Osaka City University, Osaka 588, Japan
⁴¹University of Oxford, Oxford OX1 3RH, United Kingdom
⁴²Istituto Nazionale di Fisica Nucleare, Sezione di Padova-Trento, ^{cc}University of Padova, I-35131 Padova, Italy
⁴³LPNHE, Universite Pierre et Marie Curie/IN2P3-CNRS, UMR7585, Paris, F-75252 France
⁴⁴University of Pennsylvania, Philadelphia, Pennsylvania 19104, USA
⁴⁵Istituto Nazionale di Fisica Nucleare Pisa, ^{dd}University of Pisa,
^{ee}University of Siena and ^{ff}Scuola Normale Superiore, I-56127 Pisa, Italy
⁴⁶University of Pittsburgh, Pittsburgh, Pennsylvania 15260, USA
⁴⁷Purdue University, West Lafayette, Indiana 47907, USA
⁴⁸University of Rochester, Rochester, New York 14627, USA
⁴⁹The Rockefeller University, New York, New York 10065, USA
⁵⁰Istituto Nazionale di Fisica Nucleare, Sezione di Roma 1,
⁹⁹Sapienza Università di Roma, I-00185 Roma, Italy
⁵¹Rutgers University, Piscataway, New Jersey 08855, USA
⁵²Texas A&M University, College Station, Texas 77843, USA
⁵³Istituto Nazionale di Fisica Nucleare Trieste/Udine,
I-34100 Trieste, ^{hh}University of Trieste/Udine, I-33100 Udine, Italy
⁵⁴University of Tsukuba, Tsukuba, Ibaraki 305, Japan
⁵⁵Tufts University, Medford, Massachusetts 02155, USA
⁵⁶Waseda University, Tokyo 169, Japan
⁵⁷Wayne State University, Detroit, Michigan 48201, USA
⁵⁸University of Wisconsin, Madison, Wisconsin 53706, USA
⁵⁹Yale University, New Haven, Connecticut 06520, USA
- (Dated: August 23, 2010)

We present a measurement of the top-quark width using $t\bar{t}$ events produced in $p\bar{p}$ collisions at Fermilab's Tevatron collider and collected by the CDF II detector. In the mode where the top quark decays to a W boson and a bottom quark, we select events in which one W decays leptonically and the other hadronically (lepton + jets channel). From a data sample corresponding to 4.3 fb^{-1} of integrated luminosity, we identify 756 candidate events. The top-quark mass and the mass of W boson that decays hadronically are reconstructed for each event and compared with templates of different top-quark widths (Γ_t) and deviations from nominal jet energy scale (Δ_{JES}) to perform a simultaneous fit for both parameters, where Δ_{JES} is used for the *in situ* calibration of the jet energy scale. By applying a Feldman-Cousins approach, we establish an upper limit at 95% confidence level (CL) of $\Gamma_t < 7.6 \text{ GeV}$ and a two-sided 68% CL interval of $0.3 \text{ GeV} < \Gamma_t < 4.4 \text{ GeV}$ for a top-quark mass of $172.5 \text{ GeV}/c^2$, which are consistent with the standard model prediction. This is the first direct measurement of Γ_t to set a lower limit with 68% CL.

PACS numbers: 14.65.Ha, 13.85.Qk, 12.15.Ff

The top quark is the heaviest known elementary par-

*Deceased

†With visitors from ^aUniversity of Massachusetts Amherst, Amherst, Massachusetts 01003, ^bIstituto Nazionale di Fisica Nucleare, Sezione di Cagliari, 09042 Monserrato (Cagliari), Italy, ^cUniversity of California Irvine, Irvine, CA 92697, ^dUniversity of California Santa Barbara, Santa Barbara, CA 93106 ^eUniversity of California Santa Cruz, Santa Cruz, CA 95064, ^fCERN, CH-1211 Geneva, Switzerland, ^gCornell University, Ithaca, NY 14853, ^hUniversity of Cyprus, Nicosia CY-1678, Cyprus, ⁱUniversity College Dublin, Dublin 4, Ireland, ^jUniversity of Fukui, Fukui City, Fukui Prefecture, Japan 910-0017, ^kUniversidad Iberoamericana, Mexico D.F., Mexico, ^lIowa State University, Ames, IA 50011, ^mUniversity of Iowa, Iowa City, IA 52242, ⁿKinki University, Higashi-Osaka City, Japan 577-8502, ^oKansas State University,

Manhattan, KS 66506, ^pUniversity of Manchester, Manchester M13 9PL, England, ^qQueen Mary, University of London, London, E1 4NS, England, ^rMuons, Inc., Batavia, IL 60510, ^sNagasaki Institute of Applied Science, Nagasaki, Japan, ^tNational Research Nuclear University, Moscow, Russia, ^uUniversity of Notre Dame, Notre Dame, IN 46556, ^vUniversidad de Oviedo, E-33007 Oviedo, Spain, ^wTexas Tech University, Lubbock, TX 79609, ^xIFIC(CSIC-Universitat de Valencia), 56071 Valencia, Spain, ^yUniversidad Tecnica Federico Santa Maria, 110v Valparaiso, Chile, ^zUniversity of Virginia, Charlottesville, VA 22906, ^{aa}Yarmouk University, Irbid 211-63, Jordan, ⁱⁱOn leave from J. Stefan Institute, Ljubljana, Slovenia,

ticle, whose large mass results in the largest decay width and hence the shortest lifetime of the quarks in the standard model (SM). A precise measurement of the top-quark width Γ_t is a good test of the standard model, whose prediction at the Born level [1] is affected by the Quantum Chromodynamics (QCD) radiative corrections of order 10% [2], as well as by electroweak corrections [3, 4], which are of order 1.5%. The dominant decay mode of the top quark in the SM produces a W boson and a bottom quark (b). Neglecting terms with V_{ts} and V_{td} , which are two of the Cabibbo-Kobayashi-Maskawa (CKM) matrix elements, and terms of order m_b^2/m_t^2 , α_s^2 , and $(\alpha_s/\pi)M_W^2/m_t^2$, where m_b , m_t , and M_W denote the masses of the bottom quark, top quark, and W boson respectively and α_s is the strong coupling constant, the next-to-leading-order top-quark width predicted in the SM is [1, 2]:

$$\Gamma_t = |V_{tb}|^2 \times \frac{G_F m_t^3}{8\pi\sqrt{2}} \times \left(1 - \frac{M_W^2}{m_t^2}\right)^2 \times \left(1 + 2\frac{M_W^2}{m_t^2}\right) \times \left[1 - \frac{2\alpha_s}{3\pi} \left(\frac{2\pi^2}{3} - \frac{5}{2}\right)\right], \quad (1)$$

where G_F is the Fermi coupling constant and V_{tb} is another one of the CKM matrix elements. If we take $|V_{tb}|$ to be unity, given a top-quark mass of $172.5 \text{ GeV}/c^2$ [5] the above equation gives a value of Γ_t of 1.3 GeV , corresponding to a lifetime of $5 \times 10^{-25} \text{ s}$.

A deviation from the SM could indicate a significant contribution of non-SM particles. Novel top-quark decay modes motivated by the large top-quark mass include decay to a charged Higgs $t \rightarrow b + H^+$ [6–9], decay to its supersymmetric scalar partner stop plus neutralinos [10, 11], and flavor changing neutral current (FCNC) top-quark decays [12]. Therefore, the direct measurement of Γ_t is a general way to constrain such processes.

The first direct measurement of Γ_t was carried out with an integrated luminosity of 1 fb^{-1} of CDF data in the lepton + jets channel [13] and set an upper limit on $\Gamma_t < 13.1 \text{ GeV}$ at 95% confidence level (CL). Here we increase the data set to 4.3 fb^{-1} in the same channel, apply a kernel density estimation (KDE) [14, 15] technique to make templates, and determine the jet energy scale (JES) calibration *in situ*. In addition, the methods for setting and incorporating systematic effects are different from the previous analysis. We are able to set a lower bound on the top-quark width at 68% CL for the first time.

CDF II [16] is a general-purpose detector located at one of the two collision points along the ring of the Tevatron accelerator. A silicon microstrip tracker and a cylindrical drift chamber in a 1.4 T magnetic field serve as a charged particle tracking system. Electromagnetic and hadronic calorimeters are used to measure the energies of electrons and jets. Outside the calorimeters lie drift chambers which can detect muons. We employ a cylindrical coordinate system for the detector where θ

and ϕ are the polar and azimuthal angles, respectively, with respect to the proton beam, and pseudorapidity $\eta \equiv -\ln \tan(\theta/2)$. Transverse energy and momentum are defined as $E_T = E \sin \theta$ and $p_T = p \sin \theta$, respectively, where E and p are energy and momentum.

Top quarks decay almost exclusively to a W boson and a b quark through the weak interaction in the SM. We identify $t\bar{t}$ events in the lepton + jets channel, where one W boson decays to a charged lepton and neutrino, and the other W boson decays to two quarks. The $t\bar{t}$ candidate events used in this analysis are collected by triggers that identify at least one high- p_T lepton. Offline these events are selected by requiring a high- E_T electron or high- p_T muon (E_T or $p_T > 20 \text{ GeV}$), large missing transverse energy \cancel{E}_T ($\cancel{E}_T > 20 \text{ GeV}$) due to the undetected neutrino from the leptonic W decay, and at least four hadronic jets. Jets are reconstructed with the JETCLU [17] cone algorithm using a cone radius of $\Delta R = \sqrt{\Delta\eta^2 + \Delta\phi^2} = 0.4$. To determine if a jet comes from a b quark, the SECVTX [18] algorithm, which makes use of the transverse decay length of a b quark inside a jet (b -tag), is applied. At least one jet must be identified as b -tagged. We divide the candidate events into those with one b -tagged jet and those with two or more b -tagged jets in order to improve the usage of statistical information, since these two kinds of events have different signal-to-background ratios. When an event has one b -tagged jet (b -jet), we require this event to have exactly four jets each with $E_T > 20 \text{ GeV}$; when an event contains two or more b -jets, three jets are required to have $E_T > 20 \text{ GeV}$, the fourth must have $E_T > 12 \text{ GeV}$, and the event is allowed to have extra jets. More details about event selection criteria can be found in [19].

Monte Carlo (MC) simulated signal samples are created for a fixed top-quark mass of $172.5 \text{ GeV}/c^2$ by the PYTHIA version 6.216 [20] event generator and have different values of Γ_t between 0.1 GeV and 30 GeV , as well as various values of Δ_{JES} , which is the difference between the JES effects in MC simulation and data and has a range from $-3.0 \sigma_c$ to $+3.0 \sigma_c$, where σ_c is the CDF JES fractional uncertainty [21]. The overall rate of background events with one W boson and additional jets ($W + \text{jets}$), the dominant background process, is determined using data after subtracting off the rate of events coming from QCD multi-jet production (non- W events), and separating out a MC based estimate for electroweak processes (EWK) such as diboson ($WW/WZ/ZZ$) and single-top production. The fractions of $W + \text{jets}$ events with heavy flavor quarks (Wc , $Wc\bar{c}$, and $Wb\bar{b}$ events) are determined from MC simulated samples. The rate with which events with a W boson and light flavor quarks contain a misidentified b -jet is determined using data samples triggered by the presence of jets. Table I summarizes the background compositions, and the selection criteria for determining the background rates are described in [22]. Diboson backgrounds are modeled with PYTHIA version 6.216 [20] and $W + \text{jets}$ by ALPGEN version 2.10' [23], with jet fragmentation modeled by PYTHIA

TABLE I: The sources and expected numbers of background events in the lepton + jets channel, and the number of events observed for single b -tag and double b -tag samples after event selection, χ^2 cut, and boundary cuts.

	single b -tag	double b -tag
W + jets	85.6 ± 21.8	9.8 ± 2.9
non- W	24.5 ± 20.6	2.4 ± 1.8
EWK	10.2 ± 0.8	2.4 ± 0.2
Total background	120.2 ± 30.0	14.6 ± 3.4
Observed events	542	214

version 6.325 [20]. Single-top production events are generated by MADEVENT [24] and its fragmentation is modeled with PYTHIA version 6.409 [25].

We use a template method to extract Γ_t . Two observables, the reconstructed top-quark mass (m_t^{reco}) and the invariant mass of the two jets from the hadronically decaying W boson (m_{jj}), are built for each data event or MC simulated event (both signal and background). With the assumption that the leading (most energetic) four jets in the detector come from the four primary quarks of $t\bar{t}$ events in lepton + jets channel, there are 12 possible assignments of jets to quarks in each event. The neutrino transverse momentum is calculated from the imbalance of the transverse momentum of decaying products, jets and lepton, in the event, with unclustered energy taken into account, which is the energy in the calorimeter not associated with the lepton or one of the four leading jets. We use a χ^2 -like kinematic fitter [26] (with 9 degrees of freedom) to fit top-quark mass for each assignment and take m_t^{reco} from the assignment that has the lowest χ^2 . Events with $\chi^2 > 9.0$ are removed from the sample to reject poorly reconstructed events. We also apply boundary cuts on m_t^{reco} ($110 \text{ GeV}/c^2 < m_t^{reco} < 350 \text{ GeV}/c^2$) and m_{jj} ($50 \text{ GeV}/c^2 < m_{jj} < 115 \text{ GeV}/c^2$ for single b -tag events and $50 \text{ GeV}/c^2 < m_{jj} < 125 \text{ GeV}/c^2$ for double b -tag events) and normalize the probability density func-

tions (p.d.f.) in these regions. m_{jj} is calculated as an invariant mass of two non- b -tagged jets, which provides the closest value to the world average W boson mass of $80.40 \text{ GeV}/c^2$ [27]. The estimated number of background events and observed number of events from a data set corresponding to an integrated luminosity of 4.3 fb^{-1} after event selection, χ^2 cut, and boundary cuts are listed in Table I.

After event reconstruction, we use the MC simulated models of signal and background processes to build two-dimensional p.d.f.'s that give the probabilities of observing a pair of value of m_t^{reco} and m_{jj} , given some Γ_t and Δ_{JES} . We employ a KDE that associates to each data point a function (called a kernel function) and uses a non-parametric method to estimate the p.d.f.'s of a random variable by summing all the kernel functions, without any assumption about functional form of the p.d.f.'s. Figure 1 shows the p.d.f.'s of m_t^{reco} with different Γ_t and

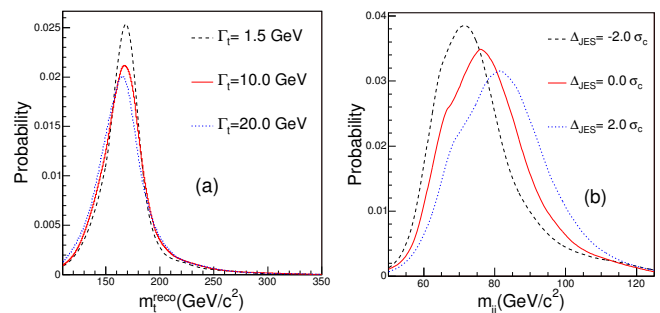


FIG. 1: (a) Probability density functions of m_t^{reco} from double b -tag events for MC simulated samples of different values of Γ_t ; (b) p.d.f.'s of m_{jj} from double b -tag events for MC simulated samples of different values of Δ_{JES} .

the m_{jj} with various Δ_{JES} from a full simulation. We compare the distributions of data with signal and background p.d.f.'s using an unbinned maximum likelihood fit [28], where the likelihood function \mathcal{L} is defined as

$$\mathcal{L} = e^{-\frac{\Delta_{JES}^2}{2\sigma_c^2}} \times \frac{(n_s + n_b)^N e^{-(n_s + n_b)}}{N!} \times e^{-\frac{(n_{b0} - n_b)^2}{2\sigma_{n_{b0}}^2}} \times \prod_{i=1}^N \frac{n_s P_s(m_t^{reco}, m_{jj}; \Gamma_t, \Delta_{JES}) + n_b P_b(m_t^{reco}, m_{jj}; \Delta_{JES})}{n_s + n_b}, \quad (2)$$

where n_s and n_b are the expected number of signal and background events, n_{b0} is the *a priori* estimate for the expected number of background events and N is the total number of observed events, and P_s and P_b are the p.d.f.'s for signal and background respectively. The first term in Eq. (2) is a prior that constrains the Δ_{JES} to the nominal CDF value within its uncertainty, σ_c . The second term makes the equation an extended likelihood, meaning that the number of signal and background events obey Pois-

son statistics. The third term constrains n_b within its uncertainty $\sigma_{n_{b0}}$ to improve sensitivity. P_s and P_b in the fourth term, which are obtained from the KDE, are used to describe signal and background events. We minimize the negative logarithm of the likelihood using MINUIT [29] to extract the top-quark width. The fitting to Δ_{JES} reduces the JES systematic effect on Γ_t and thus improves the sensitivity to the top width.

We set the limit(s) on Γ_t via the Feldman-Cousins

method [30] which determines the confidence intervals. The ordering parameter for MC simulated samples that appears in [30] is defined here as $\Delta\chi^2 = \chi_{input}^2 - \chi_{min}^2$, where $\chi^2 = -2\log(\mathcal{L})$ (different from the χ^2 mentioned in event reconstruction), χ_{min}^2 is the minimal χ^2 value and χ_{input}^2 is the χ^2 at the real value of parameters Γ_t and Δ_{JES} of the MC simulated sample. We project the likelihood function \mathcal{L} onto the Γ_t axis [31]. For each value of Γ_t we run 6,000 pseudo-experiments that generate a distribution of $\Delta\chi^2$ from which we calculate a critical value $\Delta\chi_c^2$ so that 95% of the pseudo-experiments have a $\Delta\chi^2$ falling in the interval $[0, \Delta\chi_c^2]$. With MC simulated samples of 21 different top widths Γ_t we get a profile of $\Delta\chi_c^2(\Gamma_t)$. When analyzing the data we obtain $\Delta\chi^2(\Gamma_t|data) = -2\log(\mathcal{L}) + 2\log(\mathcal{L}_0)$, where \mathcal{L}_0 is the maximum likelihood value of data fitting, then $\Delta\chi^2(\Gamma_t|data)$ is compared with $\Delta\chi_c^2(\Gamma_t)$ and the accepted interval of Γ_t is all points such that

$$\Delta\chi^2(\Gamma_t|data) < \Delta\chi_c^2(\Gamma_t). \quad (3)$$

From the above method we obtain a purely statistical upper limit on Γ_t at 95% CL, $\Gamma_t < 6.7$ GeV and a two-sided limit of $0.5 \text{ GeV} < \Gamma_t < 3.9 \text{ GeV}$ at 68% CL.

We examine systematic effects by comparing MC simulated experiments in which we vary several parameters within their uncertainties. As seen from Table II, the dominant systematic effects come from jet energy resolution and color reconnection (CR) [32], which is a rearrangement of the underlying color structure of an event from its simplest configuration. For jet energy resolution effect, we compare jet energy resolution between data and MC simulated samples using one photon + one jet events and smear jet energy with the difference between data and MC simulated samples. We study the effect of CR by using PYTHIA version 6.4 with different tunes (with and without CR) [33] and evaluate the difference. As one can see in this table, the systematic effect due to JES is very small because we perform an *in situ* JES calibration. Other smaller systematic effects include those due to MC generator, the parton distribution function, and multiple hadron interaction, details of which can be found in [5, 33]. The total change of measured Γ_t due to these systematic effects is 1.6 GeV. We studied the dominant systematic uncertainties by varying top-quark width, and found no significant dependence of systematic effects on different top-quark widths

To incorporate systematic effects into the limit(s) on Γ_t we use a convolution method for folding systematic effects into the likelihood function [34, 35]. We convolve the likelihood function with a Gaussian p.d.f. that has a width equal to 1.6 GeV and is centered at 0. With this new likelihood function we apply the Feldman-Cousins approach and find an upper limit of $\Gamma_t < 7.6$ GeV at 95% CL. Using the same approach we are also able to set a two-sided bound for Γ_t at 68% CL: $0.3 \text{ GeV} < \Gamma_t < 4.4 \text{ GeV}$. Figure 2(a) shows the data fit from the two-dimensional likelihood function with the statistical

TABLE II: Summary of changes in measured Γ_t due to systematic effects.

Systematic Sources	$\Delta\Gamma_{top}$ (GeV)
Jet energy resolution	1.1
Color Reconnection	0.9
Generator	0.4
Residual JES	0.3
Parton distribution functions	0.3
Multiple Hadron Interaction	0.3
gluon gluon fraction	0.3
Initial/Final state radiation	0.2
Lepton energy scale	0.2
<i>b</i> jet energy	0.2
Background shape	0.1
Total systematic effect	1.6

uncertainty. The overlap of the $\Delta\chi_c^2(\Gamma_t)$ profile and the one-dimensional data fit that comes from the projection of the two-dimensional likelihood function is shown in Fig. 2(b), on which the point(s) of interception gives the limit(s) of Γ_t .

In conclusion, a top-quark width measurement in the lepton + jets channel is presented. Using a data set corresponding to an integrated luminosity of 4.3 fb^{-1} collected by CDF and an *in situ* JES calibration, we derive for the first time a direct two-sided bound on the top-quark width. Assuming a top-quark mass $M_{top} = 172.5 \text{ GeV}/c^2$, we find $0.3 \text{ GeV} < \Gamma_t < 4.4 \text{ GeV}$ at 68% CL, which corresponds to a life time of $1.5 \times 10^{-25} \text{ s} < \tau_t < 2.2 \times 10^{-24} \text{ s}$. For a typical quark hadronization time scale of $3.3 \times 10^{-24} \text{ s}$ (corresponding to 200 MeV) [36, 37], our result supports top-quark decay before hadronization. An upper limit $\Gamma_t < 7.6 \text{ GeV}$ at 95% CL is also set, which is consistent with the standard model. This measurement is statistically limited and its dominant systematic uncertainties are likely to be reducible with improved data statistics. The precision of this measurement, therefore, will continue to improve over the course of Run II of the Tevatron.

We thank the Fermilab staff and the technical staffs of the participating institutions for their vital contributions. This work was supported by the U.S. Department of Energy and National Science Foundation; the Italian Istituto Nazionale di Fisica Nucleare; the Ministry of Education, Culture, Sports, Science and Technology of Japan; the Natural Sciences and Engineering Research Council of Canada; the National Science Council of the Republic of China; the Swiss National Science Foundation; the A.P. Sloan Foundation; the Bundesministerium für Bildung und Forschung, Germany; the World Class University Program, the National Research Foundation of Korea; the Science and Technology Facilities Council and the Royal Society, UK; the Institut National de Physique Nucleaire et Physique des Particules/CNRS; the Russian Foundation for Basic Research; the Minis-

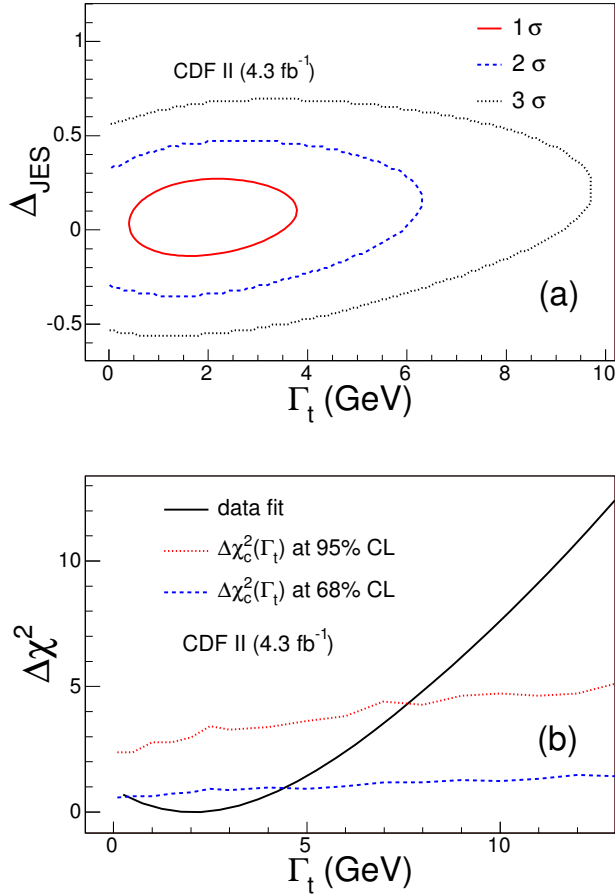


FIG. 2: (a) Contours of the two-dimensional negative log likelihood function from data fit. The three different contours represent different values of $-\log(\mathcal{L})$: 0.5, 2.0, and 4.5. Systematic effects are not included here. (b) Overlap of the $\Delta\chi_c^2(\Gamma_t)$ profile and the data fit that comes from projection of the two-dimensional data fit onto the Γ_t axis, the intersection of which gives a limit(s) on Γ_t . Systematic effects are included in the plots, both for 68% and 95% CL.

terio de Ciencia e Innovación, and Programa Consolider-Ingenio 2010, Spain; the Slovak R&D Agency; and the Academy of Finland.

-
- [1] M. Jezabek and J.H. Kuhn, Phys. Rev. **D 48**, 1910 (1993).
[2] M. Jezabek and J.H. Kuhn, Nucl. Phys. **B 314**, 1 (1989).
[3] A. Denner and T. Sack, Nucl. Phys. **B 358**, 46 (1991).
[4] G. Eilam, R. R. Mendel, R. Migneron, and A. Soni, Phys. Rev. Lett. **66** 3105 (1991).
[5] T. Aaltonen *et al.* (CDF Collaboration), Phys. Rev. **D 79**, 092005 (2009).
[6] V. Barger and J. L. Hewett, Phys. Rev. **D 41**, 3421 (1990).
[7] F. Abe *et al.* (CDF Collaboration), Phys. Rev. **D 54**, 735 (1996).
[8] V. M. Abazov *et al.* (D0 Collaboration), Phys. Rev. Lett. **88**, 151803 (2002).
[9] T. Aaltonen *et al.* (CDF Collaboration), Phys. Rev. Lett. **103**, 101803 (2009).
[10] K. Hikasa and M. Kobayashi, Phys. Rev. **D 36**, 724 (1987).
[11] C. S. Li, J. M. Yang, and B. Q. Hu, Phys. Rev. **D 48**, 5425 (1993).
[12] J. L. Diaz-Cruz, M. A. Perez, G. Tavares-Velasco, and J. J. Toscano, Phys. Rev. **D 60**, 115014 (1999).
[13] T. Aaltonen *et al.* (CDF Collaboration), Phys. Rev. Lett. **102**, 042001 (2009).
[14] K. Cranmer, Comput. Phys. Commun. **136**, 198 (2001); arXiv:hep-ex/0011057.
[15] T. Aaltonen *et al.* (CDF Collaboration), Phys. Rev. **D 79**, 092005 (2009).
[16] D. Acosta *et al.* (CDF Collaboration), Phys. Rev. **D 71**, 032001 (2005).
[17] F. Abe *et al.* (CDF Collaboration), Phys. Rev. **D 45**, 1448 (1992).

- [18] T. Affolder *et al.* (CDF Collaboration), Phys. Rev. **D 64**, 032002 (2001).
- [19] D. Acosta *et al.* (CDF Collaboration), Phys. Rev. **D 71**, 052003 (2005).
- [20] T. Sjostrand, L. Lonnblad and S. Mrenna, arXiv:hep-ph/0108264v1.
- [21] A. Bhatti *et al.* (CDF Collaboration), Nucl. Instr. Methods Phys. Res., Sect. A **566**, 375 (2006).
- [22] T. Aaltonen *et al.* (CDF Collaboration), Phys. Rev. Lett. **105**, 012001 (2010).
- [23] M. L. Mangano, M. Moretti, F. Piccinini, R. Pittau and A.D. Polosa, J. High Energy Phys. 07 (2003) 001.
- [24] F. Maltoni and T. Stelzer, J. High energy Phys. 02 (2003) 027.
- [25] T. Sjostrand, S. Mrenna and P. Skands, J. High Energy Phys. 05 (2006) 026.
- [26] A. Abulencia *et al.* (CDF Collaboration), Phys. Rev. **D 73**, 032003 (2006).
- [27] C. Amsler *et al.* (Particle Data Group), Phys. Lett. **B 667**, 1 (2008).
- [28] R. Barlow, Nucl. Instrum. Methods A **297**, 496 (1990).
- [29] F. James and M. Roos, Comput. Phys. Commun. **10**, 343 (1975).
- [30] G. Feldman and R. Cousins, Phys. Rev. **D 57**, 3873 (1998).
- [31] W. Press, S. Teukolsky, W. Vetterling, and B. Flannery, *Numerical Recipes: The Art of Scientific Computing*, (Cambridge University Press, New York, 1992), p. 963.
- [32] D. Wicke and P. Z. Skands, Eur. Phys. J **C52**,133 (2007).
- [33] T. Aaltonen *et al.* (CDF Collaboration), Phys. Rev. **D 81**, 031102 (2010).
- [34] J. Berger, B. Liseo, and R. Wolpert, Statist. Sci. **14**, 1 (1999).
- [35] L. Demortier, *Proceedings of the Conference on Advanced Statistical Techniques in Particle Physics, Durham, 2002*, (Institute for Particle Physics Phenomenology, University of Durham, UK, 18-22 March 2002); IPPP/02/39 (2002), p. 145.
- [36] I. Bigi, Y. Dokshitzer, V. Khoze, J. Huhn and P. Zerwas, Phys. Lett. **B 181**, 157 (1986).
- [37] L. H. Orr and J. L. Rosner, Phys. Lett. **B 246**, 221 (1990).